Susceptibility Mapping Using Regularization Enabled Harmonic Artifact Removal

Hongfu Sun[1] and Alan H. Wilman[1]
[1]*Biomedical Engineering, University of Alberta, Edmonton, Alberta, Canada*

PURPOSE: Quantitative susceptibility mapping (QSM) is being promoted as a means to quantify brain iron. However, the inversion from field map (phase imaging) to susceptibility distribution is ill-conditioned, meaning errors such as background artifacts in the field map can be substantially amplified and severely distort the resulting susceptibility map. Therefore, an effective removal of the background artifact is a prerequisite for successful QSM. In this study, an improved technique based on the SHARP method (1) is proposed to remove the field artifact more effectively and further enhance the accuracy of susceptibility mapping.

THEORY: As exploited in the SHARP method (1), the mean value property (2) can be used to remove the harmonic background field component (3) by performing a convolution: $M((\delta-\rho)\otimes B_{total}) = M((\delta-\rho)\otimes B_{local})$, where ρ is a nonnegative symmetric normalized kernel; δ denotes the Dirac function; and M defines the ROI as the brain volume, but is further eroded by the radius of ρ due to the violation of the harmonic condition whenever ρ overlaps with the brain edge. To express in the Fourier domain for computing efficiency: $MF^{-1}CFB_{local} = MF^{-1}CFB_{total}$ [1], where F is the Fourier transform matrix, C is the kernel (δ-ρ) after Fourier transform. Since Eq. [1] is underdetermined due to zeros in M and C, the B_{local} solution is not unique. In the original SHARP method, Eq. [1] is first relaxed at the ROI boundary by abandoning M from the local field term, and then solved with singular value decomposition. In our new method, Tikhonov regularization (4) is used to solve Eq. [1], and this method is referred to as Regularization Enabled SHARP (RESHARP). In RESHARP, the local field with the least-norm is chosen specifically as the desired solution, since the susceptibility difference between air and water/tissue is one order of magnitude larger than the inter-tissue variation due to brain iron; hence the background field is assumed to fit the majority of the induced total field. To achieve this, the constrained minimization model is converted to a well-developed unconstrained minimization problem using the method of Lagrange multiplier, by adding the Tikhonov regularization term (L2 norm of the solution) to the data fidelity term (Eq. [1]), and balancing with the Lagrange multiplier: $\min_{B_{local}} \|MF^{-1}CFB_{local} - MF^{-1}CFB_{total}\|_2^2 + \lambda\|B_{local}\|_2^2$, where $\|\cdots\|_2^2$ denotes the sum of squares; λ is the Lagrange multiplier to be set such that the norm of the local field is minimal subject to data fidelity within expected error tolerance.

METHODS: Simulation and human brain experiments were performed. A modified 3D Shepp-Logan susceptibility phantom (128^3 pixels) was created numerically, with five ellipsoid structures (0.05, 0.1, 0.15, 0.2 and 0.3 ppm) and a sphere air cavity (9.4 ppm) inside, surrounded by background air (9.4 ppm) outside. This phantom was used for field forward calculations. Three-dimensional multiple gradient-echo datasets covering the whole head were acquired at 4.7T from five healthy volunteers (age: 48±3 yrs). The acquisition parameters were: FOV = 25.6×16×16 cm; spatial resolution = 1×1×2 mm; bandwidth = 352 Hz/voxel; TR = 40 ms; TEs = 3/7/11/15/19 ms; flip angle = 10°. Both SHARP and RESHARP were implemented to remove background artifacts from the field maps, followed by susceptibility inversions using L1 norm regularization approach (5,6). The radius of ρ was set to 5 pixels for simulation and 5 mm for in vivo. The truncation level for SHARP was set to 0 for simulation and 0.05 for in vivo. The regularization parameter for RESHARP was set to 0 for simulation, and 5×10^{-3} for in vivo.

RESULTS: As seen from the simulation results (Fig. 1): The filtered field map from SHARP (Fig. 1d) displays alternating bright-dark patterns at the boundary, while that from RESHARP (Fig. 1f) is free of these artifacts. The relative filtered field map error is 2.2% for SHARP and 1.5% for RESHARP. The susceptibility map obtained from the SHARP result (Fig. 1e) displays large intensity variation within the ellipsoids (of constant susceptibility in the model); while susceptibility obtained from RESHARP (Fig. 1g) displays greater uniformity in these structures. Linear regressions (Fig. 1) of the measured mean susceptibilities versus the original model susceptibilities for the five ellipsoids yield a slope of 1.09 for SHARP and 1.01 for RESHARP. Standard deviation of susceptibility measurements within each ellipsoid is much smaller for RESHARP with relative error of 6.5% than SHARP of 49% accounting all the ellipsoids.

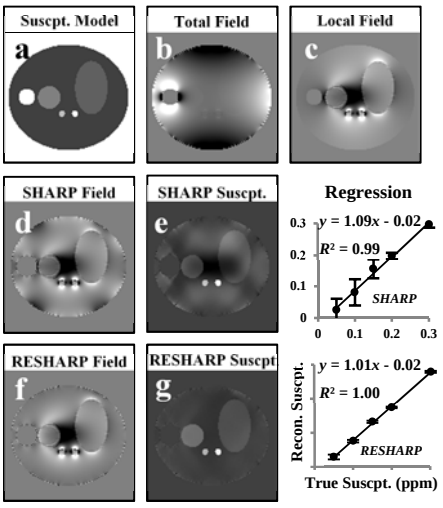

Figure 1: The field-forward susceptibility simulation results of SHARP and RESHARP.

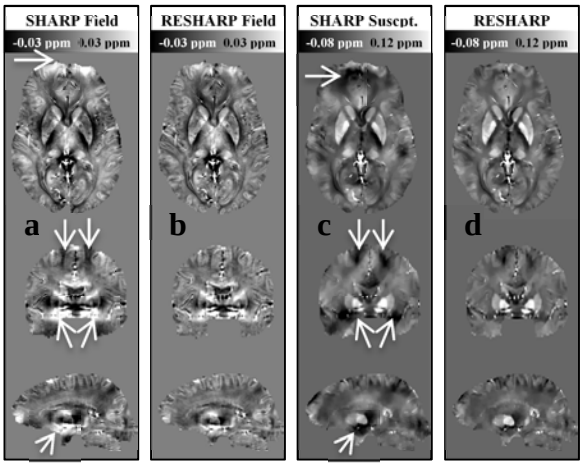

Figure 2: SHARP and RESHARP results of both the local field maps and susceptibility maps on a 45 year old male.

As seen from the in vivo human brain results (Fig. 2): Artifacts present in the SHARP field map (indicated by the white arrows in Fig. 2a) are concentrated at the boundaries of the brain, while the field map obtained from RESHARP (Fig. 2b) show artifacts substantially suppressed or completely removed in the corresponding areas. The susceptibility map calculated from the SHARP local field (Fig. 2c) shows residual streaking and severe artifact, as indicated by the white arrows, evidently resulting from residual background artifact remaining in the field map. Susceptibility maps obtained from RESHARP results (Fig. 2d) exhibit reduced artifact and better tissue contrast, with distinct delineation of the deep grey matter structures, such as the globus pallidus (GP), putamen (PU), caudate (CN), red nucleus (RN) and substantia nigra (SN).

Average susceptibilities of above deep grey matter structures from five healthy male subjects using RESHARP and SHARP are listed in Table 1. Mean values from both are similar, with SHARP on average 0.017 ppm larger than RESHARP. However, the standard deviations (SD) of the five mean measures from RESHARP are substantially smaller than those from SHARP for all structures, meaning that the RESHARP measurements are more consistent across subjects.

Table 1: Susceptibility measurements of deep grey matter structures.

Region	SHARP Δχ ± SD (ppm)	RESHARP Δχ ± SD (ppm)
GP	0.214 ± 0.161	0.197 ± 0.005
SN	0.191 ± 0.026	0.173 ± 0.020
RN	0.147 ± 0.037	0.130 ± 0.028
PU	0.121 ± 0.023	0.110 ± 0.013
CN	0.106 ± 0.033	0.082 ± 0.025

DISCUSSION: The SHARP method solves the local field solution by relaxing the Eq.[1] at the boundary, followed by truncated singular value decomposition, hence the fidelity of the equation is violated at the boundary; as a result, the solution is not accurate near the boundary. RESHARP seeks the least-norm solution by employing Tikhonov regularization, without violating the equation at the boundary. Hence, RESHARP should be more robust in this region than SHARP. This agrees with our findings from both the simulation and in vivo: SHARP induces artifacts at the ROI boundary while RESHARP can suppress or even eliminate this artifact.

CONCLUSION: An improved background field removal method (RESHARP) using Tikhonov regularization was presented. It has been shown through simulation and human brain experiments that this method is more effective at removing background field compared to original SHARP, leading to susceptibility maps with suppressed artifact and more accurate quantitative susceptibility measurements in iron-rich deep grey matter structures.

REFERENCES: [1] Schweser F et al. Neuroimage 2011;54(4):2789-807. [2] Kim J, Wong M. Complex Variables, Theory and Application: An International Journal 2005;50(14):1049-1059. [3] Li L, Leigh JS. Magn Reson Med 2004;51(5):1077-82. [4] Tikhonov AN, Arsenin VIA, John F. Solutions of ill-posed problems. 1977. [5] Liu J et al. Neuroimage 2012;59(3):2560-8. [6] Wu B et al. Magn Reson Med 2012;67(1):137-47.